Published in final edited form as:
Free Radic Biol Med. 2009 December 1; 47(11): 1640–1651. doi:10.1016/j.freeradbiomed.2009.09.011.

Sulfur mustard analog induces oxidative stress and activates signaling cascades in the skin of SKH-1 hairless mice

Arttatrana Pal,
Department of Pharmaceutical Sciences, School of Pharmacy, University of Colorado Denver, Aurora, CO 80045, USA

Neera Tewari-Singh,
Department of Pharmaceutical Sciences, School of Pharmacy, University of Colorado Denver, Aurora, CO 80045, USA

Mallikarjuna Gu,
Department of Pharmaceutical Sciences, School of Pharmacy, University of Colorado Denver, Aurora, CO 80045, USA

Chapla Agarwal,
Department of Pharmaceutical Sciences, School of Pharmacy, University of Colorado Denver, Aurora, CO 80045, USA

Jie Huang,
Department of Medicine, National Jewish Health, 1400 Jackson Street, Denver, CO 80206, USA.

Brian J. Day,
Department of Medicine, National Jewish Health, 1400 Jackson Street, Denver, CO 80206, USA.

Carl W. White, and
Pediatrics, National Jewish Health, 1400 Jackson Street, Denver, CO 80206, USA.

Rajesh Agarwal
Department of Pharmaceutical Sciences, School of Pharmacy, University of Colorado Denver, Aurora, CO 80045, USA

Abstract

Monofunctional analog of chemical warfare agent sulfur mustard (HD), 2-chloroethyl ethyl sulfide (CEES), induces tissue damage similar to HD. Herein; we studied the molecular mechanisms associated with CEES-induced skin inflammation and toxicity in SKH-1 hairless mice. Topical CEES exposure caused an increase in oxidative stress as observed by enhanced 4-hydroxynonenal (4-HNE) and 5, 5-dimethyl-2-(8-octanoic acid)-1-pyrroline N-oxide (DMPO) protein adduct formations, and an increase in protein oxidation. CEES-induced increase in the formation of 8-oxo-2-deoxyguanosine (8-OH2dG) indicated DNA oxidation. CEES exposure instigated increase in the phosphorylation of mitogen-activated protein kinases (MAPKs, ERK1/2, JNK and p38). Following CEES-exposure, a significant increase in the phosphorylation of Akt at Ser473 and Thr308 was observed as well as up regulation of its upstream effector, PDK1 in mouse skin tissue. Subsequently, CEES exposure caused activation of AP-1 family proteins, and NF-κB pathway, including phosphorylation and degradation of IκBα in addition to phosphorylation of NF-κB essential modulator (NEMO). Collectively, our results indicate that CEES induces oxidative stress and the activation of transcription factors AP-1

Corresponding author: Rajesh Agarwal, Department of Pharmaceutical Sciences, School of Pharmacy, University of Colorado Denver, 12700 E. 19th Avenue, Box C238-P15, Research-2, Aurora, CO 80045, USA; Phone: 303-724-4055, Fax: 303-724-7266, Rajesh.Agarwal@ucdenver.edu.

and NF-κB via upstream signaling pathways including MAPKs and Akt in SKH-1 hairless mouse skin. These novel molecular targets could be supportive in development of prophylactic and therapeutic interventions against HD-related skin injury.

Keywords

CEES; SKH-1 hairless mice; oxidative stress; 4-HNE; DMPO; MAPKs; AP1; Akt; NF-κB

Introduction

Sulfur mustard (HD, bis(2-chloroethyl) sulfide), is a strong vesicant and an alkylating chemical warfare agent. It was first used in World War I and has since been utilized in numerous conflicts, including the Iraq–Iran war [1,2]. Apart from inflicting injury to lungs, eyes and other organ systems, primary toxic effect of HD is on exposed skin tissue, where it induces severe damage and inflammation including erythema, edema, necrosis, vesication, ulceration and desquamation [3–6]. Detailed understanding of the molecular mechanisms involved in HD-induced skin toxicity are important for the development of effective countermeasures and therapeutics against this chemical warfare agent of mass destruction. Several reports show that HD-induced tissue toxicity is mainly due to its alkylating properties, enhanced production of inflammatory cytokines, and increased oxidative stress owing to production of damaging reactive oxygen species (ROS) [1,7–9]. Though, there are compound mechanisms implicated in HD-induced inflammation and toxicity, one of the important reported mechanisms is the depletion of glutathione (GSH) that likely leads to an increase in the production of ROS, and consequent membrane lipid peroxidation [5,7]. In addition, both direct alkylation and free radical-induced alkylation that causes protein oxidation, lipid peroxidation and DNA/RNA damage, could be involved in HD-caused skin toxicity and inflammation [7,10]. Roles of mitogen activated protein kinases (MAPKs), transcription factor NF-κB, p53, poly (ADP-ribose) polymerase (PARP), Fas calcium and calmodulin have also been suggested in the molecular mechanisms of HD-induced skin toxicity and inflammation [3,5,11–14]. However, despite extensive research attempts, complete understanding of the multiple molecular mechanisms and signaling pathways involved in HD-induced skin inflammation and injury in an efficient animal model, is still lacking. Commercially available monofunctional analog of HD, CEES, a vesicant and an alkylating agent; has been experimentally explored to gain knowledge of the mechanisms involved in HD-induced skin toxicity [15,16].

MAPKs are serine/threonine kinases phosphorylated in response to various stimuli, including stress, pro-inflammatory cytokines, UV radiation etc [17]. Mediating signal transduction from cell surface to the nucleus, the MAPKs are important pro-inflammatory mediators that also play an important role in cell survival, cellular stress, and cellular proliferation and differentiation [17]. There are three major MAPK pathways; extracellular signal regulating kinases (ERK), p38 MAP kinases, and c-jun N-terminal kinases (JNKs). ERK kinases are mainly activated by mitogenic signals, whereas JNK and p38 are predominantly activated by environmental stress such as UV radiation, inflammatory cytokines, heat shock and DNA damaging agents [18]. Individual phosphorylated MAPKs activate the MAPK/ERK kinase (MEK), mitogen-activated protein kinase kinase (MKK3/6, MKK-4, MKK-7) that are generally specific for individual MAPKs, and control diverse cellular processes [18]. Anti-apoptotic and diverse cell survival stimuli including oxidative stress also activate the phosphatidylinositol-3-kinase (PI3K/Akt) pathway that engages in the activation of various transcription factors such as NF-κB and AP-1 [19–21]. The lipid kinase PI3K is involved in the regulation of processes like transcription, migration, angiogenesis, cell growth, proliferation and apoptosis.

MAPK pathways effect the activity of AP-1, an important regulatory protein, which plays a major role in epithelial cell growth, differentiation, transformation and apoptosis [22]. This transcription factor is composed of protein dimers encoded by Fos (c-Fos, FosB, Fra-1, and Fra-2), Jun (cJun, JunD, and JunB) and activating transcription factor families (ATF-1 and ATF-2) [22,23]. The modulation of AP-1 families is mediated by MAPKs, while AP-1 is known to play an important role in the transcriptional activation of metalloproteinases (MMPs) [23]. The NF-κB transcription factor, important mediator of inflammatory responses, is a complex of homo or heterodimerization of its subunits p50, p52, RelA (p65), RelB and RelC [24]. It is sequestered in cytoplasm in an inactive condition due to association with an inhibitory protein, IκB [24]. Extracellular signals like pro-inflammatory cytokines, bacterial lipopolysaccharide, UV irradiation, carcinogenic chemicals, genotoxic anticancer agents and intracellular oxidative stress activate NF-κB via convergence on the cytoplasmic IκB kinase (IKK) complex [24, 25]. Activated IKK phosphorylates IκBα and IκBβ proteins and phosphorylated IκBα is degraded by the 26S proteosome complex in the cytoplasm [25]. As a result, free NF-κB enters into the nucleus, binds to its cognate sites in the promoter regions and activates the target genes. Small ubiquitin like modifier I (SUMO I) and the modification of NEMO/IKKγ are required for NF-κB activation [26,27].

It is reported that NF-κB and AP-1, that play a central role in mediating inflammatory responses, are downstream targets of MAPK and Akt pathways that are, in part, activated by oxidative stress [19,22,28,29]. Therefore, we hypothesize that CEES-mediated oxidative stress could activate MAPK and Akt pathways; subsequent signals from both MAPKs and Akt could congregate downstream and activate transcription factors NF-κB and AP-1 that could be important in mediating various cellular responses leading to CEES-mediated skin inflammation and injury. Our recent findings have established dose- and time-dependent quantitative inflammatory biomarkers of HD analog, CEES-induced skin injury in more resourceful SKH-1 hairless mouse model [16]. Based on this background, the present study adopted a comprehensive approach to analyze the involvement of oxidative stress and roles of MAPKs and Akt signaling, activation of their downstream transcription factors AP1 and NF-κB in CEES-induced skin inflammation and toxicity in SKH-1 hairless mouse model. The findings of this study identified useful molecular targets involved in CEES-induced skin toxicity in a single efficient *in vivo* model, providing valuable molecular markers of inflammation that could be used to identify and screen compounds to treat/prevent HD-caused skin toxicity.

Materials and Methods

Chemicals and reagents

HD analog, CEES (purity 98 %) was obtained commercially from Sigma-Aldrich Chemical Co. (St. Louis., MO). Consensus sequences of double stranded AP-1 and NF-κB oligonucleotides were purchased from Santa Cruz Biotechnology (CA, USA). The phosphorylated MEK1/2 (Ser217, 221), ERK1/2 (Thr202 and Tyr204), MKK- 4 (Ser257 and Thr261), MKK3/6 (Ser189 and Ser207), MKK-7 (Ser271 and Thr275), JNK (Thr183/ Tyr185), p38 (Thr180/ Tyr182), PDK1 (Ser241), Akt (Ser473 and Thr308), PTEN (Ser308/ Thr382/383), ATF-2 (Thr69/71) and p65 (Ser536 and Ser276), total MEK1/2, ERK1/2, JNK, p38, Akt, IκBα, PETEN and ATF-2 primary antibodies were purchased from Cell Signaling Technology (Beverly, MA, USA). Phosphorylated mouse monoclonal anti-cJun, -cFos and non-phosphorylated rabbit-anti p65, p50, cJun, cFos, Fra-1, Fra-2, Fos B, Jun B, Jun D antibodies were purchased from Santa Cruz Biotechnology (CA, USA). Mouse monoclonal anti-SUMO-1 (anti GMP1) was purchased from Zymed Laboratories (San Francisco, CA, USA). Mouse monoclonal anti-IKKγ (NEMO) was purchased from BD Pharmigen (San Jose, CA, USA). Anti-4-HNE rabbit polyclonal antibody was kind gift from Dr. Dennis Petersen

(School of Pharmacy, University of Colorado Denver, USA). Anti-DMPO nitrone polyclonal antiserum was purchased from Cayman Chemicals (Ann Arbor, MI, USA). Monoclonal anti-β-actin antibody was obtained from Santa Cruz Biotechnology (CA, USA). An anti-mouse IgG HRP-linked secondary antibody was obtained from Amersham Bioscience (UK) and anti-rabbit IgG horseradish peroxidase (HRP)-conjugated secondary antibody was obtained from Cell Signaling Technology (Beverly, MA, USA). Protein assay kit was obtained from Bio-Rad laboratory (USA) and enhanced chemiluminescence western blot detection reagents were purchased from Amersham Biotech (Piscataway, NJ, USA). [γ-^{32}P]ATP and 5X gel shift binding buffer were obtained from Promega (Madison, WI, USA).

Animals and CEES exposure

Female SKH-1 hairless mice (5 weeks old) were obtained from Charles River Laboratories (Wilmington, MA) and housed under standard conditions at the Center of Laboratory Animal Care, University of Colorado Denver, CO. The animals were acclimatized for one week before their use in experimental studies, which were carried out according to the specified protocol approved by the IACUC of the University of Colorado Denver, CO. Acetone alone or the required concentrations of CEES were diluted in acetone fresh and applied topically on the mice medial and dorsal surface of the skin in a continuously operated chemical and biological safety fume hood [16].

Experimental design

In the dose-response study, mice were exposed topically to CEES doses in the range of 0.05–2 mg in 200 μl acetone /mouse that was applied on the dorsal skin for 12 h as described earlier [16]. Briefly, a total of 50 mice were randomly divided into 10 groups; (i) control-untreated, (ii) 200 μl acetone alone/mouse (vehicle control), (iii) 0.05 mg CEES, (iv) 0.1 mg CEES, (v) 0.25 mg CEES, (vi) 0.4 mg CEES, (vii) 0.5 mg CEES, (viii) 1 mg CEES, (ix) 1.5 mg CEES, and (x) 2 mg CEES. As published in our previous study [16], time-response study employed 1 and 2 mg CEES doses, and the study time points were 3, 6, 9, 12, 24, 48, 72 and 168 h. At the end of each desired treatment, the mice were euthanized, and the dorsal skin was collected as described earlier [16,30] and snap frozen in liquid nitrogen.

Preparation of tissue lysates and western blot analysis

Subcutaneous fatty tissue was removed from each skin tissue and then whole cell extract, cytosolic and nuclear fractions were prepared as published earlier [31,32]. The protein content of the tissue extracts was determined by Lowry's method (Bio-Rad, Regents Park, New South Wales, Australia). Equal amounts of protein from the desired samples were resolved on Tris-glycine gel (8 % to 12 %), transferred to nitrocellulose membranes and blocked for 1 h with 5 % nonfat dry milk. Membranes were incubated with the appropriate concentrations of primary antibodies overnight at 4 °C, and then incubated with HRP-conjugated secondary antibody. The same membrane was reprobed with anti-β-actin antibody as loading control.

Western blot analysis for protein oxidation

For western blot analysis of oxidative modification of protein, the OxyBlot Protein Oxidation Detection kit (Chemicon International, USA) was employed following manufacturer's protocol. The protein lysate (20 μg) was denatured by adding 12 % sodium dodecyl sulfate (SDS) to a final concentration of 6 % SDS. The protein samples were derivatized by adding 2, 4-dinitrophenylhydrazine (DNPH) solution and to the aliquot designated as the negative control, derivatization-control solution instead of the DNPH solution was used for 15 min. Reaction was stopped by adding the neutralizing solution to both the samples. The derivatized samples and the negative control were loaded on the 12% sodium dodecyl sulfate (SDS)-polyacrylamide gel for electrophoresis, and blotted onto a nitrocellulose membrane. The

membrane was blocked in phosphate-buffered saline (PBS) containing 0.1 % Tween-20 (PBS-T) and 5 % non-fat dry milk for 1 h. The membrane was then incubated overnight at 4 °C with the corresponding diluted primary antibody (1: 150) in non-fat dry milk in PBS-T as described by the manufacturer. This was followed by incubating the membrane with HRP-conjugated secondary antibody (1: 300) for 1 h at room temperature in PBS-T containing 5 % non-fat dry milk. The membrane was washed in PBS-T and treated with a chemiluminescence reagent ECL detection kit (Piscataway, NJ, USA) according to the manufacturer's protocol.

Analysis of DNA oxidation in mouse skin

DNA from control and 2 mg CEES-treated skin tissue was extracted using DNeasy tissue kit (Qiagen; Valencia, CA, USA). DNA purity was measured using a Nanodrop 1000 spectrophotometer (Thermo Fisher). Roughly 6 μg purified DNA was incubated with 4 units of Nuclease P1(US Biological, Swampscott, MA) at 60°C for 20 min, then with 4 units of Alkaline Phosphatase (Sigma-Aldrich Chemical Co. St. Louis., MO) at 37°C for 60 min. The samples where then analyzed for 8-hydroxy-2-deoxyguanosine (8-OHdG) and 2-deoxyguanosine (2dG) respectively by HPLC coupled with UV and electrochemical detection (CoulArray model 5600; ESA Inc., Chelmford, MA). Mobile phase A consisting of 50 mM Sodium Acetate, pH 4.0, and mobile phase B consisting of 50 mM sodium acetate with acetonitrile 85:15 (v:v), pH 4.2 with a flow rate of 1mL/min using a gradient of 100% A for 5 min; 60% A, 40% B for 12 min; 20% A, 80% B for 5 min; and 100% A for 8 min. Analysis consisted of a 4.6 by 250 mm, C18 reverse phase column (Tosoh Bioscience, Montgomeryville, PA) with the detection of 2dG by UV and 8-OHdG using electrode potentials of 140, 200, 260, and 320 mV. The retention times for 2dG and 8-OHdG where 13.0 and 14.1 min, respectively. Concentrations were determined using an 11 point standard curve and expressed as a ratio of 8-OHdG/10^5 2dG.

Electrophoretic mobility shift assay (EMSA)

DNA binding activities of AP-1 and NF-κB were measured by EMSA as described before [32]. Briefly, EMSA was carried out using nuclear extracts prepared from CEES-treated skin tissue. AP-1 and NF-κB consensus oligonucleotides were radiolabeled with [γ-32P]ATP in the presence of T4 polynucleotide kinase in 10 X kinase buffer as per the manufacturer's protocol (Promega, Madison, WI, USA). Labeled probe was separated from free [γ-32P] ATP using G-25 Sephadex column. Nuclear extract (10 μg) was incubated with 5X gel shift binding buffer and then with ^{32}P-labeled AP1 and NF-κB probe for 20 min at 37 °C. In super shift and competition assays, nuclear extracts were incubated with anti- cFos, -cJun, -p65 and -p50 antibodies and unlabeled-oligos before adding labeled AP-1 and NF-κB oligos, respectively. The DNA-protein complexes were separated from the free [^{32}P]-oligonucleotides in native polyacrylamide gel in EMSA-buffer by electrophoresis at 150 V/40 mA for 1 h at 25 °C followed by gel drying and autoradiography.

Results

Topical CEES exposure caused an increase in lipid peroxidation

To determine whether oxidative stress results from CEES exposure, we compared the levels of 4-HNE, a biomarker of oxidative stress resulting from lipid peroxidation [33,34], in skin tissue of CEES exposed mice. A distinct dose- and time-dependent increase in the 4-HNE-adduct formation was evidenced on anti-4-HNE immunoblots of protein extracts, which revealed at least five discrete and rather broad bands between molecular masses of 6–192 kDa (Fig. 1). Strong bands indicating 4-HNE adduct formation were consistently present in lanes containing protein from skin tissue exposed to 1–2 mg CEES doses for 3–168 h as compared to relevant untreated and vehicle controls. In addition, lower levels of 4-HNE-adducted proteins

were spotted as faint, weaker, diffuse bands between approximate molecular masses of 40-31 kDa, 70-40 kDa and 83–131 kDa (Fig. 1).

Topical CEES exposure enhanced DMPO nitrone protein adduct formation

Measurement of protein radical adducts, formed as a result of oxidative stress via superoxide and hydroxyl radicals, is currently feasible with the development of spin trap immunoassay, which is an improved method over traditionally used electron paramagnetic resonance detection [35]. To investigate the formation of DMPO nitrone protein adducts in mice skin tissue, 1–2 mg doses of CEES were applied topically for 12 h, protein isolated and immunoblotting was carried out with DMPO nitrone adduct antiserum. As shown in Fig. 2, these exposures caused band-specific anti-DMPO staining. Molecular weight markers demonstrated the most intense bands of DMPO nitrone protein adducts between 40 and 83 kDa, 131 and 192 kDa. The strongest protein adduct bands were consistently present in lanes containing protein from skin tissue exposed to 1–2 mg CEES doses for 3–168 h as compared to relevant untreated and vehicle controls (Fig. 2). Weaker and diffuse bands below 31 kDa were also observed in these protein extracts (Fig. 2).

Topical CEES exposure caused an increase in protein oxidation

Recent studies have shown that UVB irradiation leads to accumulation of oxidatively modified proteins in mouse skin tissue [36]. Oxidation of certain amino acid residues of lysine, argenine, and proline leads to the production of carbonyl groups, and measure of these groups is a widely used method for determining oxidative stress [37]. Based on our results that show CEES-caused increase in the lipid peroxidation and DMPO nitrone adduct formation, we further performed immunoblot detection of carbonyl groups, added into proteins by oxidative reactions, in mouse skin tissue after CEES exposure using a specific antibody against DNPH. As shown in Fig. 3, CEES (1–2 mg) exposure for 12 h resulted in higher levels of protein oxidation that was evidenced by stronger carbonyl group bands relative to respective untreated and vehicle controls (Fig. 3). In addition, CEES exposure at 2 mg dose also caused an increase in protein oxidation in a time-dependent manner from 3–168 h of its exposure (Fig. 3).

Topical CEES exposure caused an increase in DNA oxidation

Since we observed an increase in lipid peroxidation and protein oxidation in CEES-exposed skin tissue, we next assessed whether CEES-mediated oxidative stress also caused DNA damage in the skin tissue. *In vivo* Oxidative DNA damage is commonly assessed by measuring the formation of 8-oxo-2-deoxyguanosine (8-OH2dG) by HPLC-EC [38]. DNA oxidative damage was assessed at 3, 6, 9, 12, 24 and 72 h after 2 mg CEES topical skin exposure. We observed a time-dependent increase in 8-OH2dG in skin DNA that peaked at 12 h after CEES exposure (Fig. 4). Skin DNA oxidation remained elevated up to 24 h after CEES exposure. This data further illustrates the sustained nature of oxidative stress and DNA damage due to topical CEES exposure.

Topical CEES exposure caused an increase in MAPKs phosphorylation

As we observed oxidative stress and oxidative DNA damage in CEES exposed skin tissue, we also wanted to study the involvement of MAPKs and related signaling pathways, which are known to be involved in oxidative stress related injuries [29,31,32]. The MAPKs are a family of intracellular enzymes that are significant intermediary of signal transduction pathways and are dually phosphorylated on a tyrosine/threonine in response to growth factors and stress stimuli [17]. Therefore, we explored the activity of MAPKs in CEES exposed mouse skin tissue, in both dose- and time-related studies. It is reported that in Raf/MEK/ERK pathway, Raf 1 is activated by HD that further activates MEK1/2 in keratinocytes [11]. A downstream target of Raf 1 is MEK1/2, and an increase in the phosphorylation of MEK1/2 at Ser217 and

Ser221 was seen after 12 h exposure to 1, 1.5 and 2 mg CEES doses. Highest level of MEK1/2 phosphorylation at this time point was observed after exposure to 1.5 mg without any change in total protein levels (Fig. 5A). CEES exposure at 2 mg dose resulted in a moderate increase of MEK1/2 phosphorylated protein levels at 3–9 h; however, stronger phosphorylation at later time-points of 12–168 h was observed compared to untreated and vehicle control groups (Fig. 5B). No significant change in total protein levels was seen. Based on the CEES-induced MEK1/2 activation, we next investigated whether CEES affected the ERK1/2-mediated mitogenic signal transduction pathway. As shown in Fig. 5A, compared to untreated and vehicle controls, exposure to different doses of CEES for 12 h caused strong dose-dependent activation of ERK1/2. CEES exposure at 2 mg dose for 3–6 h resulted in a low levels of ERK1/2 phosphorylation, however, stronger phosphorylation was observed at later time points of study (Fig. 5B). Total ERK1/2 levels were not altered by CEES exposure in either dose or time kinetic study.

Topical exposure of mice to 2 mg CEES for 12 h also resulted in strong phosphorylation of stress-associated MAPKs, p38 and JNK1/2 without changes in their total protein levels (Fig. 5C). Comparable activation of p38 was observed at different time points after exposure to 2 mg CEES. As shown in Fig. 5D, compared to untreated and vehicle controls, CEES exposure at 2 mg resulted in phosphorylation of p38 starting at 6 h that remained constant through 72 h but again declined 168 h after exposure, without any change in the total protein levels. Under similar treatment conditions, CEES exposure resulted in no detectable increase in the levels of JNK1/2 protein phosphorylation at 3–9 h, that increased from 12 h and was stronger at later time points and declined at 168 h of exposure, though the total level of JNK was unaltered (Fig. 5D). An upstream target of p38 and JNK1/2, MKK4, was seen to be phosphorylated at Ser257 and Thr261 at 12 h exposure to 2 mg CEES dose (Fig. 5C), and its phosphorylation at this dose increased from 6–72 h (Fig. 5D) as compared to respective untreated and vehicle controls. The other upstream kinases, which cause the activation of p38 and JNK1/2, are MKK3/6 and MKK7. Interestingly, phosphorylation of MKK3/6 at Ser189/207 or of MKK7 at Ser271 and Thr275 was not detected in the CEES dose- and time-response studies.

Topical CEES treatment caused an increase in Akt and PDK 1 phosphorylation

The proto-oncogene Akt is a serine/threonine kinase involved in regulation of cell survival and apoptosis and is activated by a variety of extracellular signals [20]. We explored the role of endogenous Akt and its upstream kinase PDK1 activity in CEES-mediated signaling in mouse skin tissue. Phosphorylation of PDK 1 at Ser241 increased after 12 h of exposure to 1, 1.5, and 2 mg doses of CEES (Fig. 6A). In a time-response study, moderate PDK1 protein phosphorylation was observed beginning at 3 h, increasing between 12–72 h exposure as compared to untreated and vehicle controls (Fig. 6B). Further, in both dose- and time-response studies, an increase in phosphorylation of Akt at Ser473 and Thr308 was observed as compared to respective controls, which was maximum at 12–72 h after 2 mg CEES exposure (Fig. 6A and B). Total Akt protein levels were not altered by CEES exposure in both dose and time response studies.

Topical CEES exposure caused an increase in the DNA binding activity, phosphorylation and expression of AP-1 protein family

Because our studies showed CEES-induced phosphorylation of MAPKs and Akt, we next assessed their downstream targets, cJun, cFos, and ATF-2, which belong to the AP-1 and CRE-binding protein family of transcription factors [23]. First, we sought to study the stimulatory effect of CEES exposure on AP1 activation in skin tissue nuclear extracts by EMSA, assessing the DNA-binding activity of the nuclear transcription factor AP-1. Induction in the levels of nuclear AP-1 was observed between 3 and 24 h of CEES exposure (Fig. 7A). Binding activity began tapering after 24 h and continued to decline through 168 h (Fig. 7A). To identify the

activation of AP-1 family members, nuclear extracts from CEES-treated skin tissue were incubated with anti-c-Jun/anti-c-Fos or both, followed by EMSA. Results demonstrated a supershift in c-Jun but not a non-significant shift in c-Fos, suggesting that the observed AP-1 band could consist of other subunits (Fig. 7A).

We also analyzed the protein levels of c-Fos and c-Jun, members of AP-1 family by immunoblot analysis, to confirm if both or one of them was activated by CEES. As shown in Fig. 7B, 12 h exposure to 1, 1.5 and 2 mg doses of CEES as well as 2 mg exposure for 3–168 h (Fig. 7C) resulted in phosphorylation of both cJun and cFos without any noticeable change in their total protein levels. Expression of AP-1 family proteins can be differentially regulated in response to various external and internal stimuli. We next examined the effect of topical CEES exposure on the expression of members of AP-1 subunits, Jun, Fos, and ATF-2. As shown in Fig. 7D, nuclear extracts from skin exposed to 2 mg CEES dose for 12 h, showed dramatic increase in the phosphorylation of ATF2 (Thr69/71) as compared to untreated and vehicle control skin tissue. Further time-response studies revealed that this effect of CEES at 2 mg dose began at 3 h after CEES exposure, and remained more or less unchanged until 168 h (Fig. 7E). Significant dose-dependent increases in Fos B, and Fra-2 phosphorylation was evident after 12 h in mice exposed to CEES as compared to untreated and vehicle controls (Fig. 7D). At this time point, higher (1.5 and 2 mg) CEES exposures evidenced upregulated expression of Jun B, however, analogous increases in Fra-1 and Jun D were observed at all three doses of CEES (Fig. 7D). Increases in phosphorylation of these AP-1 subunits after topical CEES exposure was also observed in the time-response study (Fig. 7E). These results indicated that CEES exposure regulated Jun and Fos expressions at the transcriptional level.

Topical CEES exposure altered DNA binding activity and caused activation of NF-κB

The nuclear transcription factor NF-κB, is responsible for cellular responses to stimuli such as stress, cytokines, free radicals, UV etc [24,39] and is reported to be a potential candidate in mediating the CEES-induced cellular responses [1]. To study the stimulatory effect of CEES on NF-κB activation, we employed EMSA to examine the DNA binding activity of NF-κB in mouse skin tissue. A strong DNA-protein interaction was observed at 12 h after exposure to 1, 1.5 and 2 mg doses of CEES (Fig. 8). Similarly, in time-response study, CEES exposure also induced strong activation of NF-κB-binding activity as compared to untreated and vehicle controls (Fig. 8). This CEES-induced activation of NF-κB was seen as early as 3 h, and was sustained until 72 h after exposure. Supershift assay demonstrated the presence of both p50 and p65 proteins in nuclear extracts after CEES exposure (Fig. 8). This suggested that DNA binding complexes in SKH-1 hairless mice consisted of p50/p65 heterodimers after CEES exposure, providing additional evidence for activation of the NF-κB pathway by CEES (Fig. 8).

Since we observed a strong DNA binding activity of NF-κB transcription factor in CEES-exposed mouse skin tissue, we next determined the changes in the levels of NF-κB family proteins. Using IκBα phosphorylation and degradation as a surrogate indicator of NF-κB activation, we also found that exposure to CEES resulted in degradation of IκBα protein and subsequent activation and translocation of NF-κB (p50/p65) to the nucleus. In the dose- and time-response studies, level of phospho IκBα protein was induced by topical CEES exposure and total IκBα protein decreased accordingly (Fig. 9A and 9B). CEES exposure for 12 h resulted in phosphorylation of the p65 subunit at Ser536 and Ser276 as compared to untreated and vehicle controls (Fig. 9A). This effect began after 3 h of CEES exposure and was persistent up to 168 h (Fig. 9B). As shown in Fig. 9A, CEES exposure for 12 h increased total p50 and p65 proteins in cytosolic fractions compared to untreated and vehicle controls. Reverse effect was evidenced in the nuclear fractions, where exposure to CEES showed decreased expression of p50 protein levels compared to untreated and vehicle controls (Fig. 9A). Parallel to cytosolic

p50 expression, total p65 protein levels in nuclear fractions increased after exposure to CEES for 12 h (Fig. 9A). In a time response study, an overall increase in both cytosolic and nuclear p50 protein was noted at 3–168 h of CEES exposure. However, the relative nuclear and cytoplasmic expression of p65 was varied over time (Fig. 9B). These results suggest that CEES exposure modulates p50 and p65 expression at multiple levels.

Oxidative stress may be critical for induction of NEMO sumoylation [27]. Based on these reports, we examined whether CEES exposure could modulate NEMO sumoylation and NF-kB activation. As shown in Fig. 9C, an increase in the phosphorylation of NEMO at Ser85 was observed in nuclear fractions after exposure of skin tissue to CEES for 12 h. In a time response study, CEES exposure at 2 mg dose for 3–12 h resulted in strong expression and nuclear accumulation of phosphorylated NEMO protein. However, at the later time-points of exposure (24–48 h), neither phosphorylation nor accumulation was observed. This effect recurred at 72–168 h after exposure relative to untreated and vehicle controls (Fig. 9D). In addition, at similar time points, the expression of phospho-and total NEMO increased in cytosolic fractions after exposure to CEES (Fig. 9C and D).

Discussion

Our knowledge of molecular mechanisms associated with both HD- and CEES-induced skin injuries, e.g. inflammation and toxicity is limited. This could be attributed, in part, to the inadequacy of efficient animal models for evaluation of these mechanisms. This has deterred the development of effective medical countermeasures and treatments against HD-mediated skin injury. In the present study, we show the involvement of oxidative stress and subsequent roles of MAPKs and Akt signaling pathways followed by transcription factors AP-1 and NF-κB in CEES-induced inflammatory response and skin injury in single efficient SKH-1 hairless mouse skin model.

Apart from direct alkylation, reported to be the major mechanism leading to HD-caused toxicity, various studies have indicated that another important mechanism involved in the toxicity caused by HD is oxidative stress that can operate via various signal transduction pathways, and can also cause alkylation [5,10,14,40]. Most previous reports indicate formation of sulfonium and carbenium ions by HD that leads to protein, lipid and DNA alkylation provoking the activation of PARP that causes the rapid depletion of NAD+/ATP leading to cell death [1,7,13,14]. Recent reports have indicated that HD-induced ROS generation can be involved in alkylation as well as induce GSH depletion that leads to lipid peroxidation, apart from possible protein oxidation and DNA injury [14,38,40].

CEES, a monofunctional and less toxic analog of HD employed in this study, has been most widely exploited as valuable laboratory experimental tool to gain insight into the mechanism of action of HD [10,15,16,38]. Although, many reports have indicated the involvement of oxidative stress in HD/CEES-induced skin and other tissue injuries [1,5,38,40], most studies have been carried out in *in vitro* systems, and HD/CEES dose- and time–dependent changes in lipid peroxidation as well as protein and DNA oxidation in a suitable animal model have not been reported.

The most important feature of oxidative damage via stress signals including UVB radiation are oxidation of biomolecules including lipids, proteins and DNA [41]. Lipid peroxidation generates numerous cytotoxic degradation products such as malondialdehyde (MDA) and 4-HNE [34], and these degradation products can form covalent adducts with proteins, phospholipids and DNA in the compartments of the cells. [42,43]. Our findings show significant increase in 4-HNE-protein adducts as early as 3 h in CEES-exposed skin tissue that sustained up to 168 h and reflect increased oxidative modification of tissue proteins *in vivo*

(Table 1). Moreover, relatively few distinct bands on immunoblots suggest that only a small number of specific proteins are the major targets of 4-HNE conjugation in CEES exposed skin. The formation of these adducts in cell compartments also suggests that significant proportion of these toxicants escape detoxification in an *in vivo* system to form adducts with tissue macromolecules. This study provides the first direct *in vivo* demonstration that suggests that significant lipid peroxidation and protein modification occurs after CEES exposure in mouse skin. As known that GSH plays an important role in lipid peroxidation [44], our results also indicate that the depletion of GSH by CEES could be a key initial mechanism in CEES-induced skin toxicity.

Spin trapping using DMPO has been used earlier to detect superoxide and hydroxyl radicals via adduct formation in EPR spectra and also DNA damage caused by toxicants. In this study, we employed an improved spin trap immunoassay [35] for detection of DMPO nitrone protein adducts to identify the free radicals formed on CEES exposure of skin tissue. Our results show a significant increase in the DMPO nitrone-protein adduct formation as early as 3 h in the CEES-exposed skin tissue and reflects increased formation of superoxide and hydroxyl radicals (Table 1).

Oxidation of amino acids (lysine, arginine, and proline), leads to the formation of carbonyl derivatives that influence the biological activity of native proteins in biological systems [45]. In different *in vivo* models, a variety of studies have utilized the presence of carbonyl groups as a measure of the oxidative damage of proteins. Oxidative stress conditions allow carbonyl groups to react with DNPH and form stable hydrazone derivatives [46,47]. In the present study, CEES exposure caused an increase in the levels of protein carbonyl groups in mouse skin both in dose- and time-kinetic studies indicating *in vivo* protein oxidation.

In this study, we also demonstrated DNA oxidation in 2 mg CEES-exposed skin tissue as had been recently shown in CEES-treated human bronchial and small epithelial cells [38]. It is interesting that both in the present study and in the recent study of Gould and co-workers; detection of CEES-mediated oxidative stress was delayed and peaked at 12 h post CEES exposure. These data are consistent with the beneficial effects that antioxidants have been reported to have in CEES and HD animal models in the lung, and support their use in skin injury as well. Present study indicates that CEES-induced oxidative stress is perhaps the central feature leading to lipid peroxidation as well as protein and DNA oxidations that occur within 3 h of CEES exposure (Table 1), and plays a key role in the activation of signaling pathways and CEES-induced skin inflammation, further supporting the antioxidant therapy.

Herein, our results show that topical exposure of SKH-1 hairless mice skin to CEES resulted in marked phosphorylation of MAPKs in both dose- and time-response studies, indicating activation of MAPKs signaling pathways including ERK1/2, p38, and JNK (Table 1). These results are in agreement with a previous finding that MAPK pathways are activated by HD/CEES in keratinocytes [11] and in lungs of male guinea pigs [48], and that the inflammatory cytokines, growth factors, and oxidative stress are the stimuli for the activation of JNK and p38 [49]. The fact that CEES is capable of inducing an inflammatory response [16], makes it very plausible that CEES activates not only JNK and p38 pathways predominantly involved in response to oxidative stress, but also ERK, resulting in or contributing to, inflammation. The proteins of the MAPK family are reported to stimulate NF-κB activation [50]. The CEES-induced activation of all three MAPK signaling pathways shown here, foremost in an *in vivo* skin toxicity model, could be responsible for the reported increases in the pro-inflammatory mediators, activation of NF-κB and induction of metalloproteinases (MMPs) [1,4,51]. Therefore, MAPK signaling pathways could be key components in contributing to the CEES-induced skin inflammation observed in dose- and time response-studies in this established mouse model [16].

Akt/protein kinase B (PKB) plays a crucial role in several processes associated with survival and apoptosis [20,31]. Several studies have shown that the kinase activity of Akt is dependent upon the phosphorylation of Akt at Thr308 by PDK1 and by phosphorylation within the carboxy-terminus at Ser473 [19]. Consistent with these reports, the present study also shows CEES-induced phosphorylation of Akt at Ser473 and Thr308, indicating activation of Akt pathway in mouse skin tissue (Table 1). On the other hand, PDK1, the upstream effector of Akt engaged in responses to stress and in growth factor signaling, potentially activates Akt and protein kinase C isoenzymes [52]. Our results indicate that increased phosphorylation of PDK1 might be the key factor for the CEES-induced Akt activation. Akt pathway engages in the activation of various transcription factors such as NF-κB and AP-1 [19,20] and therefore, suggestively plays an important role in CEES-induced activation of these transcription factors and subsequent inflammatory responses.

In this study, we further examined whether CEES-induced oxidative stress can stimulate inflammatory responses via transcription factors AP-1 and NF-κB. MAPK pathways are shown to be responsible for the phosphorylation of AP-1 proteins [23,49]. In the context of CEES-caused lung injury, it has been shown in guinea pigs that CEES treatment activates AP-1 via MAPK pathway [48]. This observation is comparable to our findings in skin exposed to CEES, as CEES-caused AP-1 activation in skin tissue also correlated with the activation of MAPK proteins, as well as could be activated via CEES-induced Akt pathway. Zhong et al. [49] demonstrated that Fos and Jun proteins differ significantly in both their DNA binding and transactivation potentials as well as regulation of their target genes. Present study shows that CEES induced the activation of both c-Fos and c-Jun members of AP-1 family (Table 1). Expression of different AP1 proteins is variably regulated in response to numerous extra cellular stimuli that induce cellular stress. Since AP-1 is a homodimer or heterodimer of Fos, Jun and ATF proteins, analysis the protein levels of individual components showed increased expression of ATF-2, Jun B, Jun D, Fos B, Fra-1 and Fra-2 protein levels after CEES exposure both in dose- and time-response studies. Further investigations are reasonable to elucidate the individual contribution of AP-1 members in CEES-induced oxidative stress and skin inflammation that could be important targets for medical interventions of its toxicity. As AP-1 proteins plays an important role in cell proliferation [22,23], the CEES-induced activation of AP-1 observed here could be associated with the CEES-induced increase in epidermal cell proliferation observed as increase in proliferating cell nuclear antigen (PCNA) staining reported in our earlier study in this mouse model [16]. AP-1 also participates in the transcriptional activation of MMPs that are reported to be important mediators in HD/CEES induced skin injury and blistering as also seen in our studies (data not shown) [23,53,54].

NF-κB plays an important role in inflammation and cell proliferation, and is activated by oxidants [41]. It causes an influence on responsive proteins PCNA, iNOS, Cox-2 and other pro-inflammatory cytokines that are reported to play an important role in CEES/HD-mediated skin injury [1,3,5,55,56] A recent report indicated that HD-induced NF-κB activation in keratinocytes was associated with activation MAPK pathways [11], though a number of previous studies have reported the role of NF-κB in CEES/HD-induced skin inflammation and toxicity [5]. In the present study subsequent to MAPKs and AP-1 activation, CEES exposure also induced NF-κB activation that was preceded by subsequent IκBα phosphorylation and its degradation. Moreover, phosphorylation and subsequent degradation of inhibitory molecules of IκB protein kinases are also required for optimal RelA/NF-κB activation by targeting functional domains of NF-κB proteins themselves [11]. RelA/NF-κB is phosphorylated at Ser536 and Ser276 by a variety of kinases via various signaling pathways and in most cases, these phosphorylations enhance RelA transactivation potential. Our findings support the idea that the phosphorylation and degradation of IκBα preceded phosphorylation of RelA/ NF-κB at Ser536 and Ser276. The overall importance of the transactivating NF-κB subunit RelA for HD-induced NF-κB activation is demonstrated by exposure of RelA-deficient keratinocytes

to HD, where, no NF-κB-binding activity was observed [11]. Our results possibly imply that NF-κB-binding activity in response to CEES is dependent on RelA phosphorylation at Ser536 and Ser276, and phosphorylation of this site is essential for RelA activity in CEES exposed mouse skin.

Huang et al. [26] demonstrated that NEMO plays a pivotal role in NF-κB signaling pathways by allowing physiological regulation of the cytoplasmic IKK complex. Besides, the signal specificity is in part due to the requirement of the C-terminal ZF domain of NEMO for SUMO-1 modification and the ZF domain is essential for NF-κB activation by DNA damaging agents. It is also reported that direct attachment of SUMO-1 to NEMO is sufficient to localize NEMO to the nucleus and overcome the ZF deficiency [26]. The present study delineated the post-translational modification of NEMO and its accumulation in nucleus and later shuttling to the cytoplasm upon stress induction by CEES exposure in mouse skin tissue. This study indicates an important role of NEMO in the activation of NF-κB upon CEES exposure in skin tissue, which could be utilized as a target for medical intervention in CEES-induced skin injury.

Oxidative stress is reported as the possible first key event in HD toxicity that possibly activates the transcription factors NF-κB and AP-1 leading to pro-inflammatory gene expression and an inflammatory response [14]. Consistent with this, several antioxidants including GSH and its precursors as well as AEOL 10150 have been implicated in attenuating the skin and lung injury caused by HD/CEES [1,38]. The results of our present study are in accord with these previous findings and further assert the role of oxidative stress in HD/CEES-caused skin inflammation, injury and vesication. Though the roles of NF-κB, p53, p38, PARP, Fas and calcium pathways are reported in the HD/CEES-caused skin inflammation and injury [5], their relation to oxidative stress and the studies in a relevant single animal model that could be useful in efficacy studies have been lacking. In this regard, the results of our present study clearly support the notion that the molecular mechanism by which CEES possibly alters the transcription factors AP-1 and NF-κB leading to skin inflammatory response and injury reported in our recent study in SKH-1 hairless mouse [16], could be oxidative stress mediated activation of MAPKs and Akt following CEES exposure of mouse skin (Table 1). The well studied and reported HD/CEES-induced DNA alkylation [5,7] could also be involved in this process alongside oxidative stress that possibly causes ROS generation leading to protein and DNA oxidation and lipid peroxidation. The DMPO nitrone-protein adduct formation, indicating oxidative protein damage, in the CEES exposed skin shown herein could be due to myeloperoxidase (MPO) that produces hypochlorous acid (HOCI) in the occurrence of chloride ions and hydrogen peroxide (H_2O_2), and is found to be the possible source of DMPO-OH adduct [57]. MPO is produced mainly in the neutrophils,but also in monocytes and macrophages that are shown to infiltrate in the CEES-exposed SKH-1 hairless mouse skin tissue in our recent studies [16,58]. In diseased tissues, oxidative products of MPO have been detected that could be either via generation of HOCl that could modify both lipids and proteins, via tyrosyl radical causing lipid peroxidation, or possibly via nitrite oxidation to generate nitrating and chlorinating intermediates leading to lipid peroxidation [58]. In future, it would be important to further dissect the role of MPO alongside GSH depletion and other reported oxidative stress mechanisms in HD/CEES-induced oxidative molecular damage that might help in understanding the mechanistic aspect of this process. Furthermore, studies are also needed in future possibly using selective ROS scavengers or pathway inhibitors to establish the role of MAPKs and Akt signaling pathways together with activation of transcription factors AP-1 and NF-κB by CEES as observed in the present study, on the recently reported inflammatory responses by CEES in this mouse model [16]. The outcomes of such studies would contribute in further understanding the mechanism of HD/CEES-induced skin injury and its direct association with CEES-induced oxidative stress in mouse skin.

In summary, the findings in present study expanded our knowledge of molecular mechanisms involved in CEES-related dose- and time-dependent skin inflammatory responses reported earlier in an efficient SKH-1 hairless mouse model [16]. The results presented here show the induction of oxidative stress by CEES, possibly leading to lipid, protein and DNA oxidations interlinked with multistep complex mechanisms of CEES-mediated skin inflammation and injury (Table 1, Fig. 10). These mechanisms involve a number of signaling cascades, which suggestively engage in the production of CEES-induced pro-inflammatory mediators and advances inflammatory response (Fig. 10). Signaling pathways such as MAPKs, Akt and transcription factors like AP-1 and NF-κB could be key factors involved in the CEES-caused skin inflammatory process (Fig. 10). The valuable molecular targets explored in this study in an efficient rodent model, could be supportive in designing potential medical interventions especially contributing to the available antioxidant therapies, and can serve as valuable indicators in future therapeutic efficacy studies against HD-induced skin toxicity. Further studies are needed in future, possibly employing proteomic strategies, to identify the individual adducted and oxidized proteins indicatively formed due to CEES-induced oxidative stress in mouse skin in the present study. These findings will enhance our understanding of the CEES/HD induced protein oxidation, contributing further in strategies to develop medical countermeasures and therapy for any possible HD-induced skin injury in humans.

Acknowledgments

This work was financially supported by grant from NIH (U54 ES015678). We thank Dr. Dennis Petersen (School of Pharmacy, University of Colorado Denver, CO, USA) for providing Anti-4-HNE rabbit polyclonal antibody.

List of Abbreviations

4-HNE	4-hydroxynonenal
AP-1	activator protein 1
ATF	activating transcription factor
CEES	2-chloroethyl ethyl sulfide
DMPO	5, 5-dimethyl-2-(8-octanoic acid)-1-pyrroline N-oxide
DNPH	2, 4- dinitrophenylhydrazine
ERK	extracellular signal-regulated kinase
IKK	IkB kinase
JNK	Jun-N terminal kinase
MAPK	mitogen-activated protein kinase
MDA	malondialdehyde
MKK	mitogen activated protein kinase kinase
NEMO	NF-κB essential modulator
8-OH2dG	8-oxo-2-deoxyguanosine
PARP	poly (ADP-ribose) polymerase
PKB	protein kinase B
ROS	reactive oxygen species
HD	sulfur mustard
SUMO	small ubiquitin like modifier

References

1. Paromov V, Suntres Z, Smith M, Stone WL. Sulfur mustard toxicity following dermal exposure: role of oxidative stress, and antioxidant therapy. J Burns Wounds 2007;7:e7. [PubMed: 18091984]
2. Kehe K, Raithel K, Kreppel H, Jochum M, Worek F, Thiermann H. Inhibition of poly(ADP-ribose) polymerase (PARP) influences the mode of sulfur mustard (SM)-induced cell death in HaCaT cells. Arch Toxicol. 2007
3. Kehe K, Balszuweit F, Emmler J, Kreppel H, Jochum M, Thiermann H. Sulfur mustard research-strategies for the development of improved medical therapy. Eplasty 2008;8:e32. [PubMed: 18615149]
4. Graham JS, Chilcott RP, Rice P, Milner SM, Hurst CG, Maliner BI. Wound healing of cutaneous sulfur mustard injuries: strategies for the development of improved therapies. J Burns Wounds 2005;4:e1. [PubMed: 16921406]
5. Ruff AL, Dillman JF. Signaling molecules in sulfur mustard-induced cutaneous injury. Eplasty 2007;8:e2. [PubMed: 18213398]
6. Brodsky B, Trivedi S, Peddada S, Flagler N, Wormser U, Nyska A. Early effects of iodine on DNA synthesis in sulfur mustard-induced skin lesions. Arch Toxicol 2006;80:212–216. [PubMed: 16252085]
7. Kehe K, Szinicz L. Medical aspects of sulphur mustard poisoning. Toxicology 2005;214:198–209. [PubMed: 16084004]
8. Das SK, Mukherjee S, Smith MG, Chatterjee D. Prophylactic protection by N-acetylcysteine against the pulmonary injury induced by 2-chloroethyl ethyl sulfide, a mustard analogue. J Biochem Mol Toxicol 2003;17:177–184. [PubMed: 12815614]
9. Mukhopadhyay S, Rajaratnam V, Mukherjee S, Smith M, Das SK. Modulation of the expression of superoxide dismutase gene in lung injury by 2-chloroethyl ethyl sulfide, a mustard analog. J Biochem Mol Toxicol 2006;20:142–149. [PubMed: 16788954]
10. Brimfield AA, Mancebo AM, Mason RP, Jiang JJ, Siraki AG, Novak MJ. Free radical production from the interaction of 2-chloroethyl vesicants (mustard gas) with pyridine nucleotide-driven flavoprotein electron transport systems. Toxicol Appl Pharmacol 2009;234:128–134. [PubMed: 18977373]
11. Rebholz B, Kehe K, Ruzicka T, Rupec RA. Role of NF-kappaB/RelA and MAPK pathways in keratinocytes in response to sulfur mustard. J Invest Dermatol 2008;128:1626–1632. [PubMed: 18200059]
12. Minsavage GD, Dillman JF 3rd. Bifunctional alkylating agent-induced p53 and nonclassical nuclear factor kappaB responses and cell death are altered by caffeic acid phenethyl ester: a potential role for antioxidant/electrophilic response-element signaling. J Pharmacol Exp Ther 2007;321:202–212. [PubMed: 17204746]
13. Kehe K, Raithel K, Kreppel H, Jochum M, Worek F, Thiermann H. Inhibition of poly(ADP-ribose) polymerase (PARP) influences the mode of sulfur mustard (SM)-induced cell death in HaCaT cells. Arch Toxicol 2008;82:461–470. [PubMed: 18046540]
14. Korkmaz A, Yaren H, Topal T, Oter S. Molecular targets against mustard toxicity: implication of cell surface receptors, peroxynitrite production, and PARP activation. Arch Toxicol 2006;80:662–670. [PubMed: 16552503]
15. Han S, Espinoza LA, Liao H, Boulares AH, Smulson ME. Protection by antioxidants against toxicity and apoptosis induced by the sulphur mustard analog 2-chloroethylethyl sulphide (CEES) in Jurkat T cells and normal human lymphocytes. Br J Pharmacol 2004;141:795–802. [PubMed: 14769780]
16. Tewari-Singh N, Rana S, Gu M, Pal A, Orlicky DJ, White CW, Agarwal R. Inflammatory biomarkers of sulfur mustard analog 2-chloroethyl ethyl sulfide-induced skin injury in SKH-1 hairless mice. Toxicol Sci 2009;108:194–206. [PubMed: 19075041]
17. Thalhamer T, McGrath MA, Harnett MM. MAPKs and their relevance to arthritis and inflammation. Rheumatology (Oxford) 2008;47:409–414. [PubMed: 18187523]
18. Raman M, Chen W, Cobb MH. Differential regulation and properties of MAPKs. Oncogene 2007;26:3100–3112. [PubMed: 17496909]

19. Ozes ON, Mayo LD, Gustin JA, Pfeffer SR, Pfeffer LM, Donner DB. NF-kappaB activation by tumour necrosis factor requires the Akt serine-threonine kinase. Nature 1999;401:82–85. [PubMed: 10485710]
20. Romashkova JA, Makarov SS. NF-kappaB is a target of AKT in anti-apoptotic PDGF signalling. Nature 1999;401:86–90. [PubMed: 10485711]
21. Gu M, Dhanalakshmi S, Mohan S, Singh RP, Agarwal R. Silibinin inhibits ultraviolet B radiation-induced mitogenic and survival signaling, and associated biological responses in SKH-1 mouse skin. Carcinogenesis 2005;26:1404–1413. [PubMed: 15831527]
22. Shaulian E, Karin M. AP-1 in cell proliferation and survival. Oncogene 2001;20:2390–2400. [PubMed: 11402335]
23. Angel P, Szabowski A, Schorpp-Kistner M. Function and regulation of AP-1 subunits in skin physiology and pathology. Oncogene 2001;20:2413–2423. [PubMed: 11402337]
24. Hayden MS, Ghosh S. Signaling to NF-kappaB. Genes Dev 2004;18:2195–2224. [PubMed: 15371334]
25. Wuerzberger-Davis SM, Nakamura Y, Seufzer BJ, Miyamoto S. NF-kappaB activation by combinations of NEMO SUMOylation and ATM activation stresses in the absence of DNA damage. Oncogene 2007;26:641–651. [PubMed: 16862178]
26. Huang TT, Wuerzberger-Davis SM, Wu ZH, Miyamoto S. Sequential modification of NEMO/IKKgamma by SUMO-1 and ubiquitin mediates NF-kappaB activation by genotoxic stress. Cell 2003;115:565–576. [PubMed: 14651848]
27. Mabb AM, Wuerzberger-Davis SM, Miyamoto S. PIASy mediates NEMO sumoylation and NF-kappaB activation in response to genotoxic stress. Nat Cell Biol 2006;8:986–993. [PubMed: 16906147]
28. Wang X, Martindale JL, Liu Y, Holbrook NJ. The cellular response to oxidative stress: influences of mitogen-activated protein kinase signalling pathways on cell survival. Biochem J 1998;333(Pt 2): 291–300. [PubMed: 9657968]
29. Singh RP, Dhanalakshmi S, Agarwal C, Agarwal R. Silibinin strongly inhibits growth and survival of human endothelial cells via cell cycle arrest and downregulation of survivin, Akt and NF-kappaB: implications for angioprevention and antiangiogenic therapy. Oncogene 2005;24:1188–1202. [PubMed: 15558015]
30. Paus R, Muller-Rover S, Van Der Veen C, Maurer M, Eichmuller S, Ling G, Hofmann U, Foitzik K, Mecklenburg L, Handjiski B. A comprehensive guide for the recognition and classification of distinct stages of hair follicle morphogenesis. J Invest Dermatol 1999;113:523–532. [PubMed: 10504436]
31. Gu M, Dhanalakshmi S, Singh RP, Agarwal R. Dietary feeding of silibinin prevents early biomarkers of UVB radiation-induced carcinogenesis in SKH-1 hairless mouse epidermis. Cancer Epidemiol Biomarkers Prev 2005;14:1344–1349. [PubMed: 15894701]
32. Gu M, Singh RP, Dhanalakshmi S, Agarwal C, Agarwal R. Silibinin inhibits inflammatory and angiogenic attributes in photocarcinogenesis in SKH-1 hairless mice. Cancer Res 2007;67:3483–3491. [PubMed: 17409458]
33. Sompol P, Ittarat W, Tangpong J, Chen Y, Doubinskaia I, Batinic-Haberle I, Abdul HM, Butterfield DA, St Clair DK. A neuronal model of Alzheimer's disease: an insight into the mechanisms of oxidative stress-mediated mitochondrial injury. Neuroscience 2008;153:120–130. [PubMed: 18353561]
34. Hartley DP, Kroll DJ, Petersen DR. Prooxidant-initiated lipid peroxidation in isolated rat hepatocytes: detection of 4-hydroxynonenal- and malondialdehyde-protein adducts. Chem Res Toxicol 1997;10:895–905. [PubMed: 9282839]
35. Ramirez DC, Chen YR, Mason RP. Immunochemical detection of hemoglobin-derived radicals formed by reaction with hydrogen peroxide: involvement of a protein-tyrosyl radical. Free Radic Biol Med 2003;34:830–839. [PubMed: 12654471]
36. Vayalil PK, Mittal A, Hara Y, Elmets CA, Katiyar SK. Green tea polyphenols prevent ultraviolet light-induced oxidative damage and matrix metalloproteinases expression in mouse skin. J Invest Dermatol 2004;122:1480–1487. [PubMed: 15175040]
37. Levine RL. Carbonyl modified proteins in cellular regulation, aging, and disease. Free Radic Biol Med 2002;32:790–796. [PubMed: 11978480]

38. Gould NS, White CW, Day BJ. A role for mitochondrial oxidative stress in sulfur mustard analog 2-chloroethyl ethyl sulfide-induced lung cell injury and antioxidant protection. J Pharmacol Exp Ther 2009;328:732–739. [PubMed: 19064720]
39. Singh RP, Tyagi A, Sharma G, Mohan S, Agarwal R. Oral Silibinin Inhibits In vivo Human Bladder Tumor Xenograft Growth Involving Down-Regulation of Survivin. Clin Cancer Res 2008;14:300–308. [PubMed: 18172282]
40. Jafari M. Dose- and time-dependent effects of sulfur mustard on antioxidant system in liver and brain of rat. Toxicology 2007;231:30–39. [PubMed: 17222496]
41. Mantena SK, Katiyar SK. Grape seed proanthocyanidins inhibit UV-radiation-induced oxidative stress and activation of MAPK and NF-kappaB signaling in human epidermal keratinocytes. Free Radic Biol Med 2006;40:1603–1614. [PubMed: 16632120]
42. Toyokuni S, Miyake N, Hiai H, Hagiwara M, Kawakishi S, Osawa T, Uchida K. The monoclonal antibody specific for the 4-hydroxy-2-nonenal histidine adduct. FEBS Lett 1995;359:189–191. [PubMed: 7867796]
43. Guichardant M, Taibi-Tronche P, Fay LB, Lagarde M. Covalent modifications of aminophospholipids by 4-hydroxynonenal. Free Radic Biol Med 1998;25:1049–1056. [PubMed: 9870558]
44. Fukuda A, Osawa T, Hitomi K, Uchida K. 4-Hydroxy-2-nonenal cytotoxicity in renal proximal tubular cells: protein modification and redox alteration. Arch Biochem Biophys 1996;333:419–426. [PubMed: 8809082]
45. Stadtman ER. Protein oxidation in aging and age-related diseases. Ann N Y Acad Sci 2001;928:22–38. [PubMed: 11795513]
46. Levine RL, Stadtman ER. Oxidative modification of proteins during aging. Exp Gerontol 2001;36:1495–1502. [PubMed: 11525872]
47. Levine RL, Wehr N, Williams JA, Stadtman ER, Shacter E. Determination of carbonyl groups in oxidized proteins. Methods Mol Biol 2000;99:15–24. [PubMed: 10909073]
48. Mukhopadhyay S, Mukherjee S, Smith M, Das SK. Activation of MAPK/AP-1 signaling pathway in lung injury induced by 2-chloroethyl ethyl sulfide, a mustard gas analog. Toxicol Lett 2008;181:112–117. [PubMed: 18675330]
49. Zhong CY, Zhou YM, Douglas GC, Witschi H, Pinkerton KE. MAPK/AP-1 signal pathway in tobacco smoke-induced cell proliferation and squamous metaplasia in the lungs of rats. Carcinogenesis 2005;26:2187–2195. [PubMed: 16051644]
50. Bonvin C, Guillon A, van Bemmelen MX, Gerwins P, Johnson GL, Widmann C. Role of the amino-terminal domains of MEKKs in the activation of NF kappa B and MAPK pathways and in the regulation of cell proliferation and apoptosis. Cell Signal 2002;14:123–131. [PubMed: 11781136]
51. Dillman JF 3rd, Phillips CS, Dorsch LM, Croxton MD, Hege AI, Sylvester AJ, Moran TS, Sciuto AM. Genomic analysis of rodent pulmonary tissue following bis-(2-chloroethyl) sulfide exposure. Chem Res Toxicol 2005;18:28–34. [PubMed: 15651846]
52. Zhang P, Ng P, Caridha D, Leach RA, Asher LV, Novak MJ, Smith WJ, Zeichner SL, Chiang PK. Gene expressions in Jurkat cells poisoned by a sulphur mustard vesicant and the induction of apoptosis. Br J Pharmacol 2002;137:245–252. [PubMed: 12208782]
53. Ries C, Popp T, Egea V, Kehe K, Jochum M. Matrix metalloproteinase-9 expression and release from skin fibroblasts interacting with keratinocytes: Upregulation in response to sulphur mustard. Toxicology. 2008
54. Shakarjian MP, Bhatt P, Gordon MK, Chang YC, Casbohm SL, Rudge TL, Kiser RC, Sabourin CL, Casillas RP, Ohman-Strickland P, Riley DJ, Gerecke DR. Preferential expression of matrix metalloproteinase-9 in mouse skin after sulfur mustard exposure. J Appl Toxicol 2006;26:239–246. [PubMed: 16489579]
55. Arroyo CM, Broomfield CA, Hackley BE Jr. The role of interleukin-6 (IL-6) in human sulfur mustard (HD) toxicology. Int J Toxicol 2001;20:281–296. [PubMed: 11766126]
56. Naghii MR. Sulfur mustard intoxication, oxidative stress, and antioxidants. Mil Med 2002;167:573–575. [PubMed: 12125850]
57. Janzen EG, Jandrisits LT, Barber DL. Studies on the origin of the hydroxyl spin adduct of DMPO produced from the stimulation of neutrophils by phorbol-12-myristate-13-acetate. Free Radic Res Commun 1987;4:115–123. [PubMed: 2854101]

58. Brennan ML, Anderson MM, Shih DM, Qu XD, Wang X, Mehta AC, Lim LL, Shi W, Hazen SL, Jacob JS, Crowley JR, Heinecke JW, Lusis AJ. Increased atherosclerosis in myeloperoxidase-deficient mice. J Clin Invest 2001;107:419–430. [PubMed: 11181641]

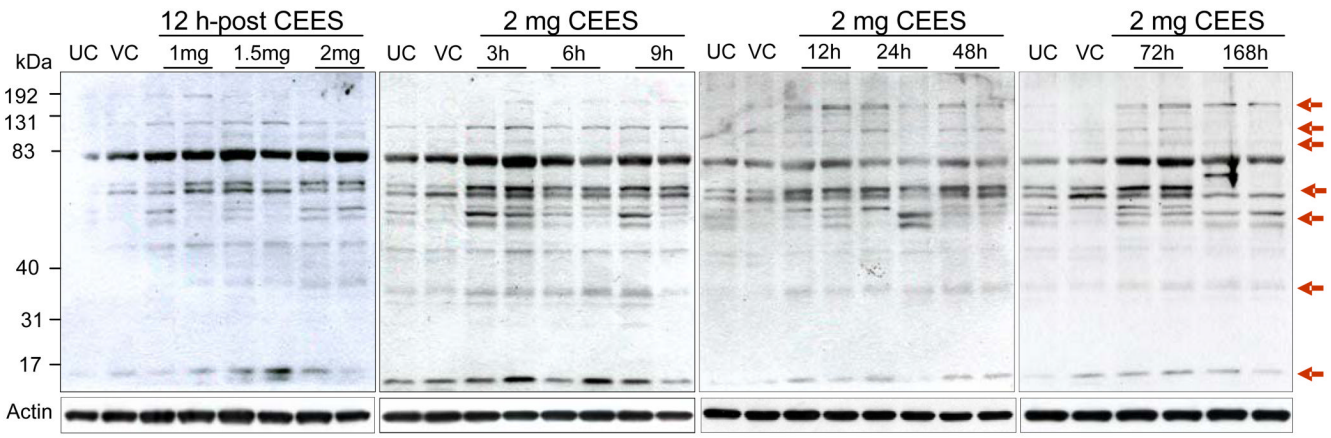

Fig. 1.

Effect of topical CEES exposure on 4-HNE-adducted protein modifications in SKH-1 hairless mouse skin. Mice were treated topically with different doses of CEES or acetone alone, and the dorsal skin was collected at specific time points as detailed under Materials and Methods. Skin epidermis samples from both dose- and time-response studies were homogenized in lysis buffer, and lysates were subjected to SDS-PAGE and immunoblotted with anti-4-HNE antibody (1:2000) as described under Materials and Methods. After exposure to X-ray film, the membranes were stripped and reprobed with β-actin. The gels are representative of two animals in each dose- and time-response study. UC, untreated control; VC, vehicle control.

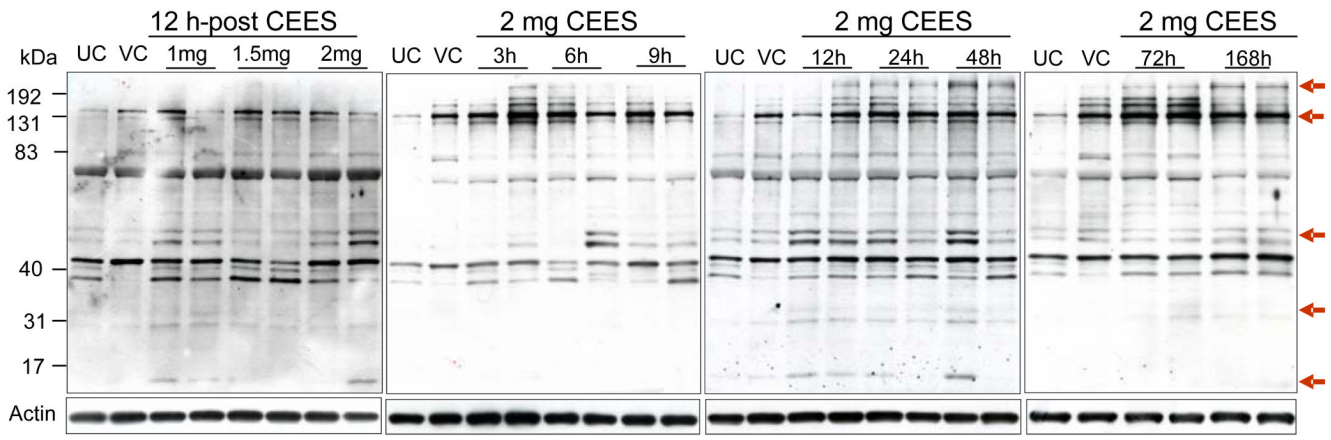

Fig. 2.

Effect of topical CEES exposure on DMPO nitrone protein adducts formation in SKH-1 hairless mouse skin. Mice were treated topically with different doses of CEES or acetone alone, and the dorsal skin was collected at specific time points as detailed under Materials and Methods. Skin epidermis samples from both dose- and time-response studies were homogenized in lysis buffer, and lysates were subjected to SDS-PAGE and immunoblotted with anti-DMPO antibody (1:1000) as described under Materials and Methods. After exposure to X-ray film, the membranes were stripped and reprobed with β-actin. The gels are representative of two animals in each dose- and time-response study. UC, untreated control; VC, vehicle control.

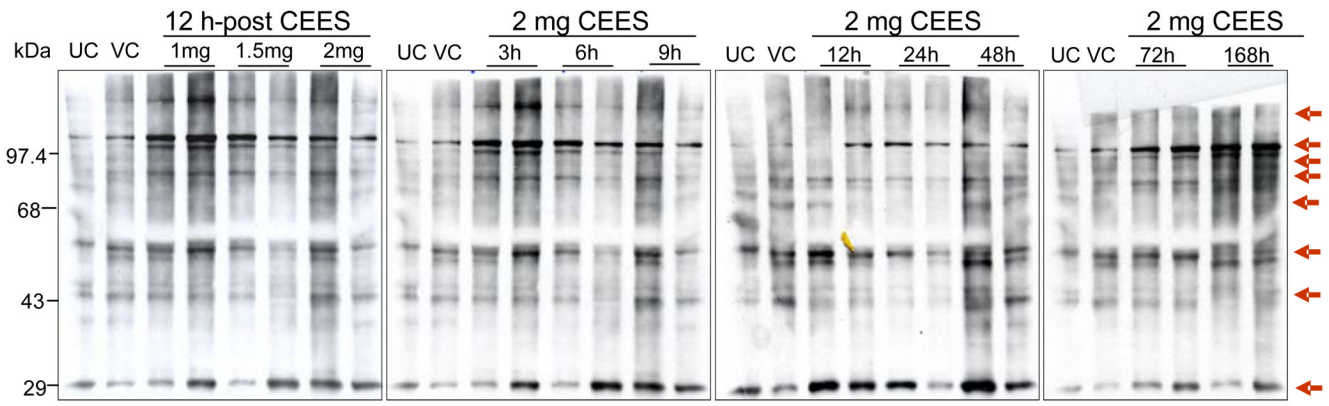

Fig. 3.

Effect of topical CEES exposure on protein oxidation in SKH-1 hairless mouse skin. Mice were treated topically with different doses of CEES or acetone alone, and the dorsal skin was collected at specific time points as detailed under Materials and Methods. Skin epidermis samples from both dose- and time-response studies were homogenized in lysis buffer, and lysates were subjected to western blot analysis for protein oxidation as described under Materials and Methods. Twenty μg of protein extracts were incubated with DNPH, subsequently electrophoresed by SDS-PAGE, blotted onto a nitrocellulose membrane, and incubated with polyclonal rabbit anti-DNPH antibody, as detailed under Material and Methods. The gels are representative of two animals in each dose- and time-response study. UC, untreated control; VC, vehicle control.

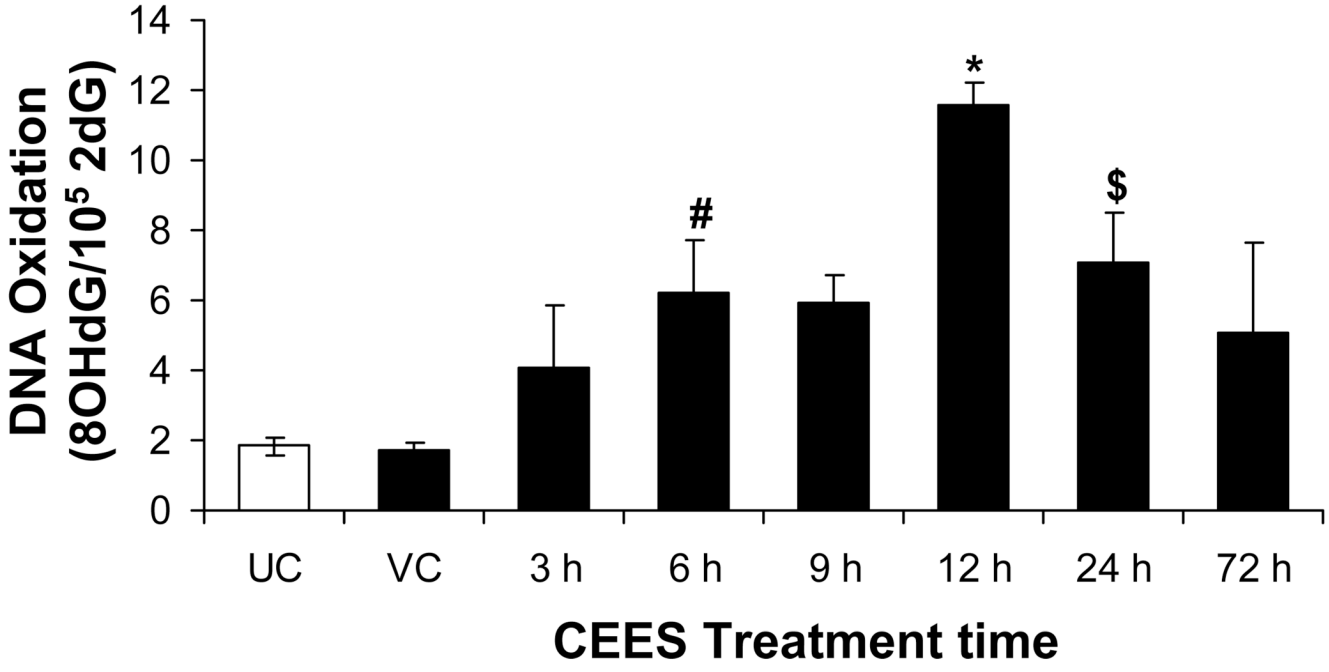

Fig. 4.

Effect of topical CEES exposure on DNA oxidation in SKH-1 hairless mouse skin. Mice were treated topically with 2 mg of CEES or acetone alone, and the dorsal skin was collected at specific time points as detailed under Materials and Methods. Skin tissue DNA from time-response study was extracted and 8-oxo-2-deoxyguanosine (8-OH2dG) was measured by HPLC-EC as described under Materials and Methods. Data was reported as the ratio of 8-OH2dG/10^5 2dG. *, $p<0.001$; $, $p<0.02$; #, $p<0.05$ as compared to untreated control group (n=3–5). UC, untreated control; VC, vehicle control.

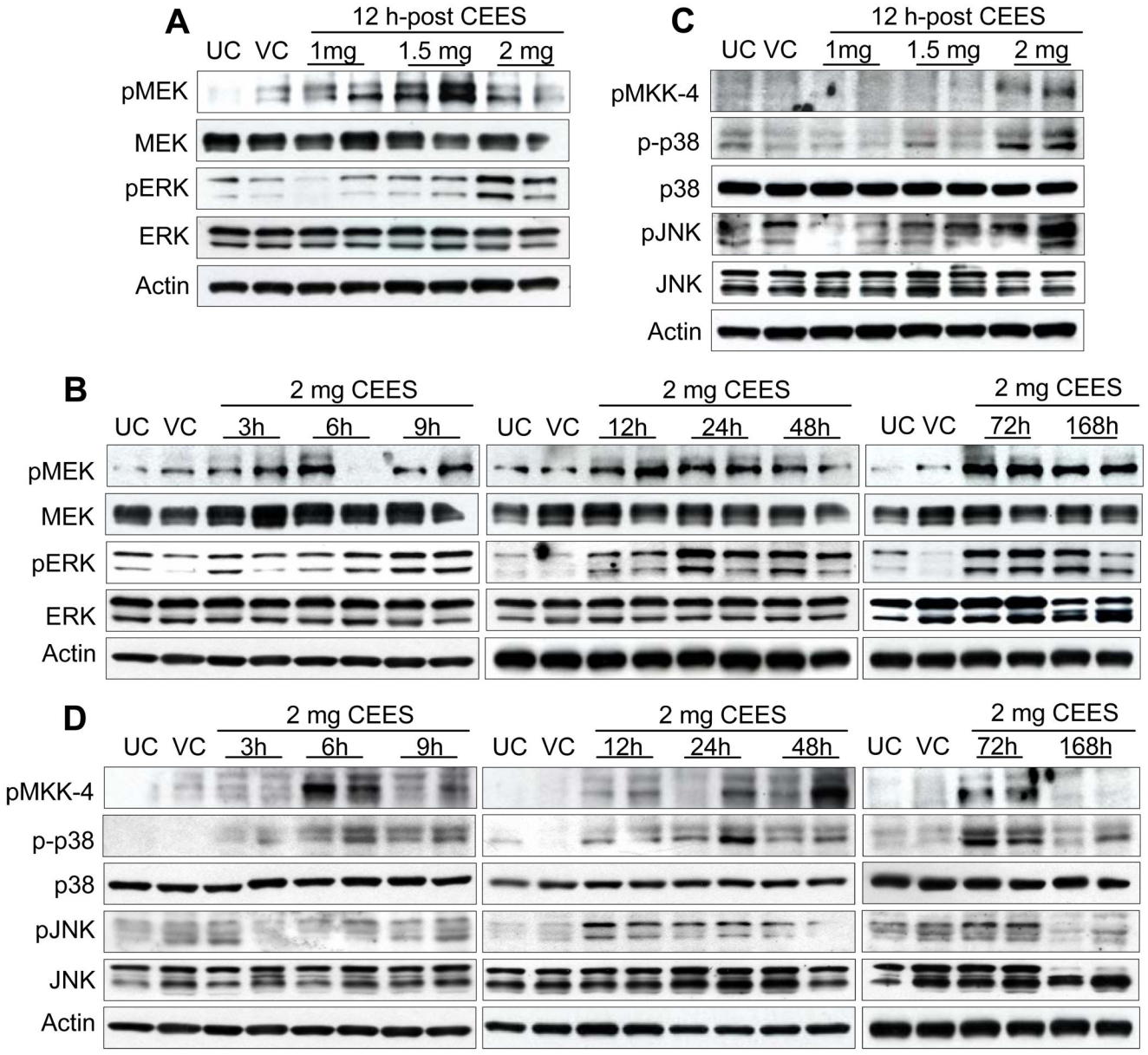

Fig. 5.

Effect of topical CEES exposure on phosphorylation of MAPKs in SKH-1 hairless mouse skin. Mice were treated topically with different doses of CEES or acetone alone, and the dorsal skin was collected at specific time points as detailed under Materials and Methods. Western blot analysis was carried out after 12 h treatment for phospho- and total MEK1/2, ERK1/2 (A), and phospho- MKK-4, phospho- and total p38, and JNK1/2 (C) using specific antibodies, as described in Materials and Methods. In time response study, skin samples were collected 3 to 168 h post-acetone alone or 2 mg CEES treatment and the MAPKs were analyzed similar to dose-response study (B and D). The membranes were stripped and reprobed with β-actin as a loading control. The results are representative of two animals in each dose- and time-response study. UC, untreated control; VC, vehicle control.

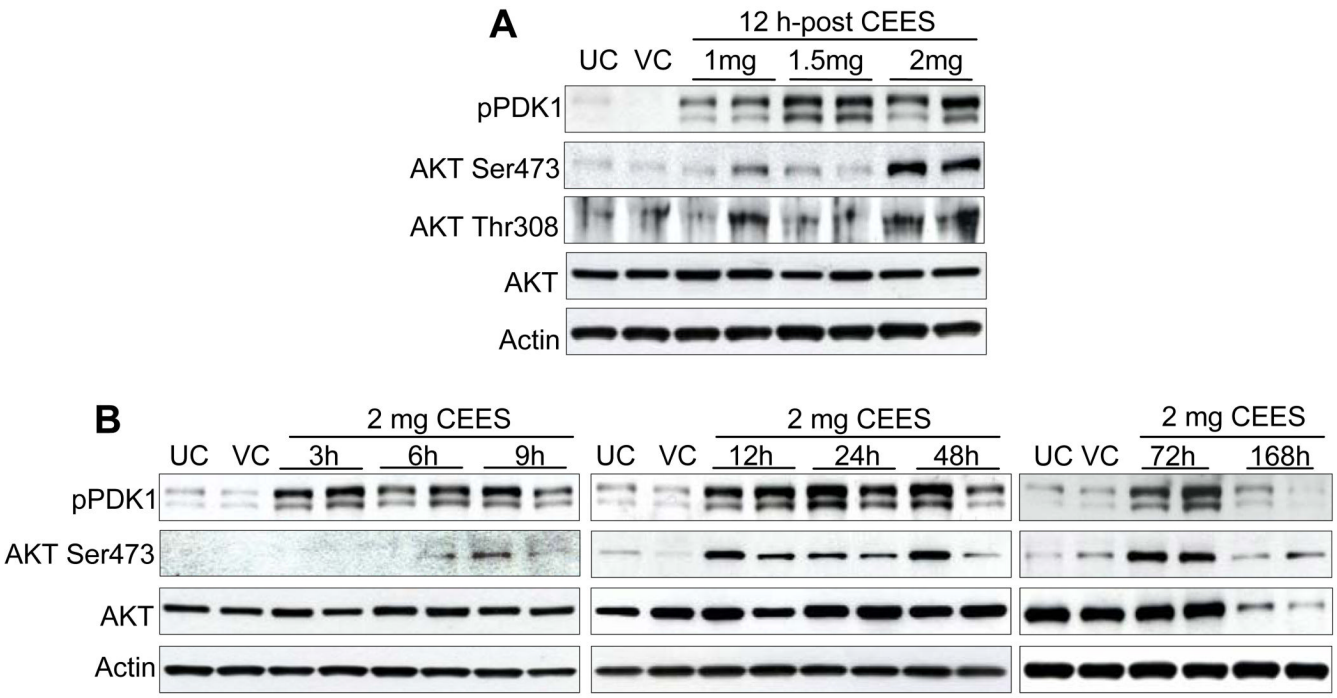

Fig. 6.

Effect of topical CEES exposure on phosphorylation of PDK1 and Akt in SKH-1 hairless mouse skin. Mice were treated topically with different doses of CEES or acetone alone, and the dorsal skin was collected at specific time points as detailed under Materials and Methods. Western blot analysis was carried out for phospho-PDK1, and phospho- and total Akt in dose-response post 12 h treatment (A) and in time-response study employing 2 mg CEES (B). The membranes were probed with phosphorylated and total antibodies followed by peroxidase-conjugated appropriate secondary antibody as detailed under Materials and Methods. After exposure to X-ray film, the membrane was stripped and reprobed with β-actin as loading control. The results are representative of two animals in each dose- and time-response study. UC, untreated control; VC, vehicle control.

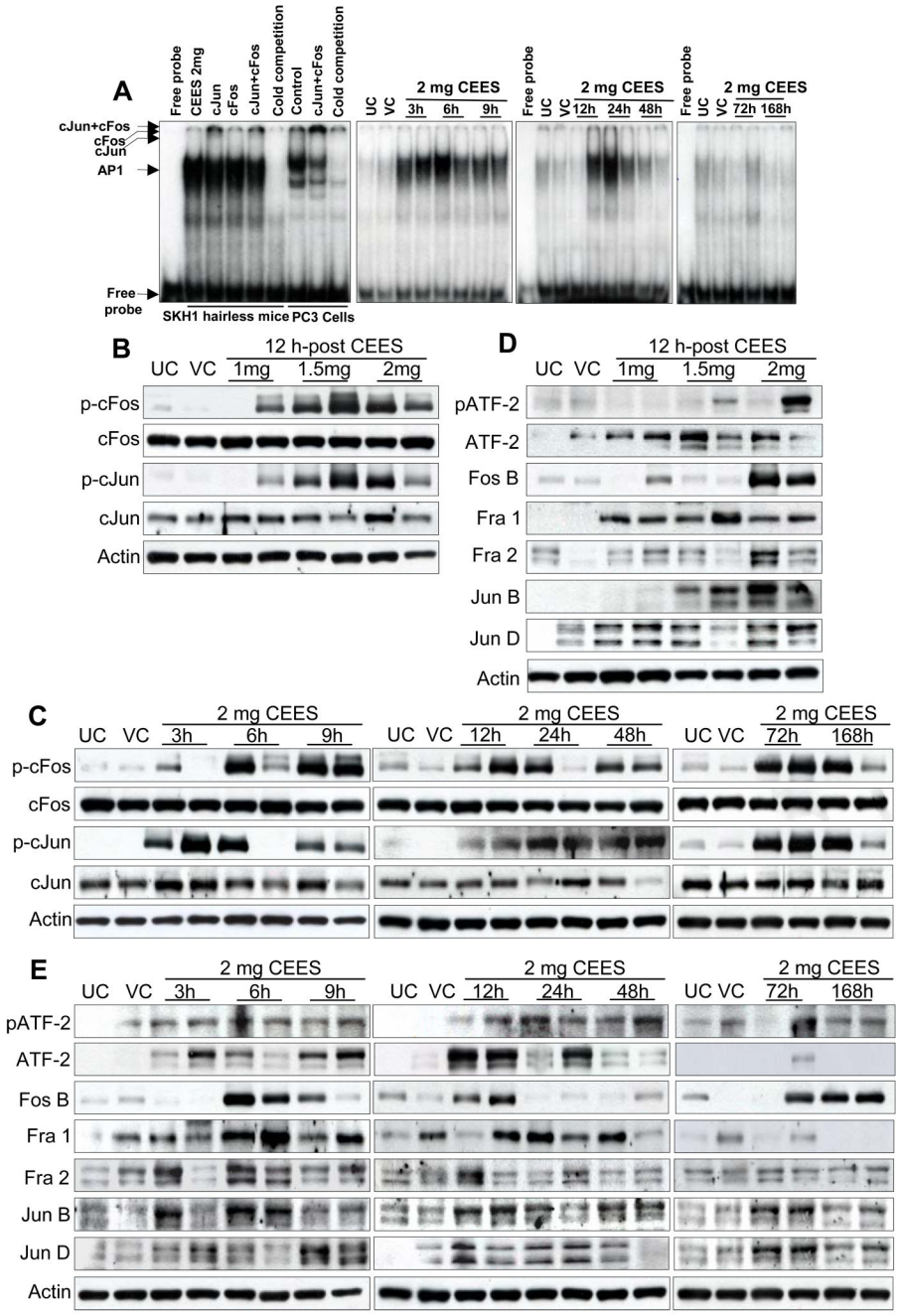

Fig. 7.

Effect of topical CEES exposure on activation of AP-1 family proteins in SKH-1 hairless mouse skin. Mice were treated topically with different doses of CEES or acetone alone, and the dorsal skin was collected at specific time points as detailed under Materials and Methods. Nuclear lysates were subjected to DNA binding activity by EMSA, for competition with cold AP1 consensus oligo, and super shift assay was conducted as described under Materials and Methods (A). Western blot analysis was done after 12 h treatment for phospho- and total cFos and cJun (B), and phospho- and total ATF-2, Fos B, Fra-1, Fra-2, Jun B, Jun D (D). These AP1 family proteins were similarly analyzed in time response study (C and E) employing 2 mg CEES as described under Materials and Methods. The membranes were stripped and reprobed with β-

actin as loading control. The results are representative of two animals in each dose- and time-response study. UC, untreated control; VC, vehicle control.

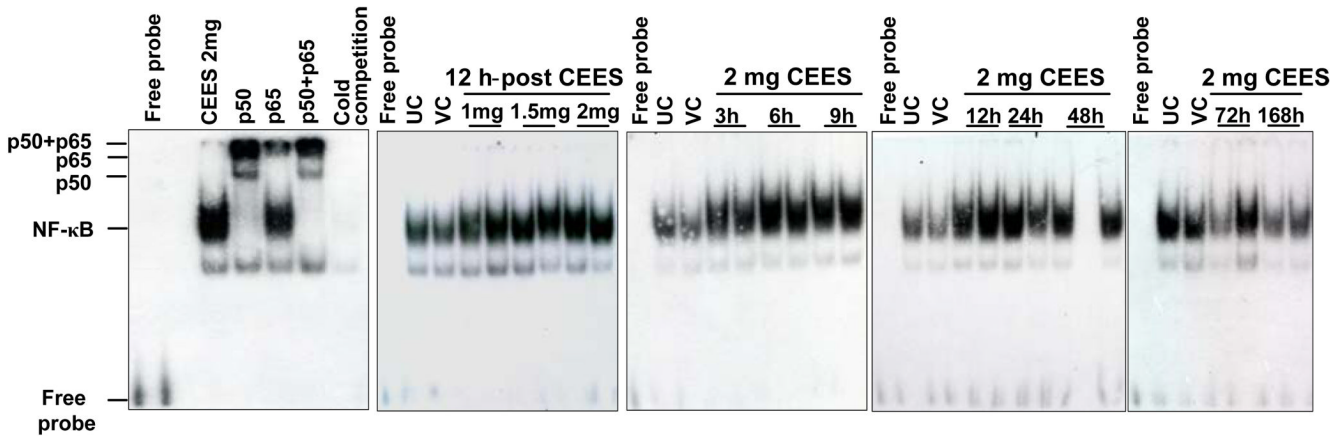

Fig. 8.

Effect of topical CEES exposure on DNA binding activity of NF-κB in SKH-1 hairless mouse skin. Mice were treated topically with different doses of CEES or acetone alone, and the dorsal skin was collected at specific time points as detailed under Materials and Methods. Nuclear extracts were subjected to DNA-binding activity in both dose- and time-response study by EMSA for competition with cold NF-κB consensus oligo and the super shift was conducted as described under Materials and Methods. The results are representative of two animals in each dose- and time-response study. UC, untreated control; VC, vehicle control.

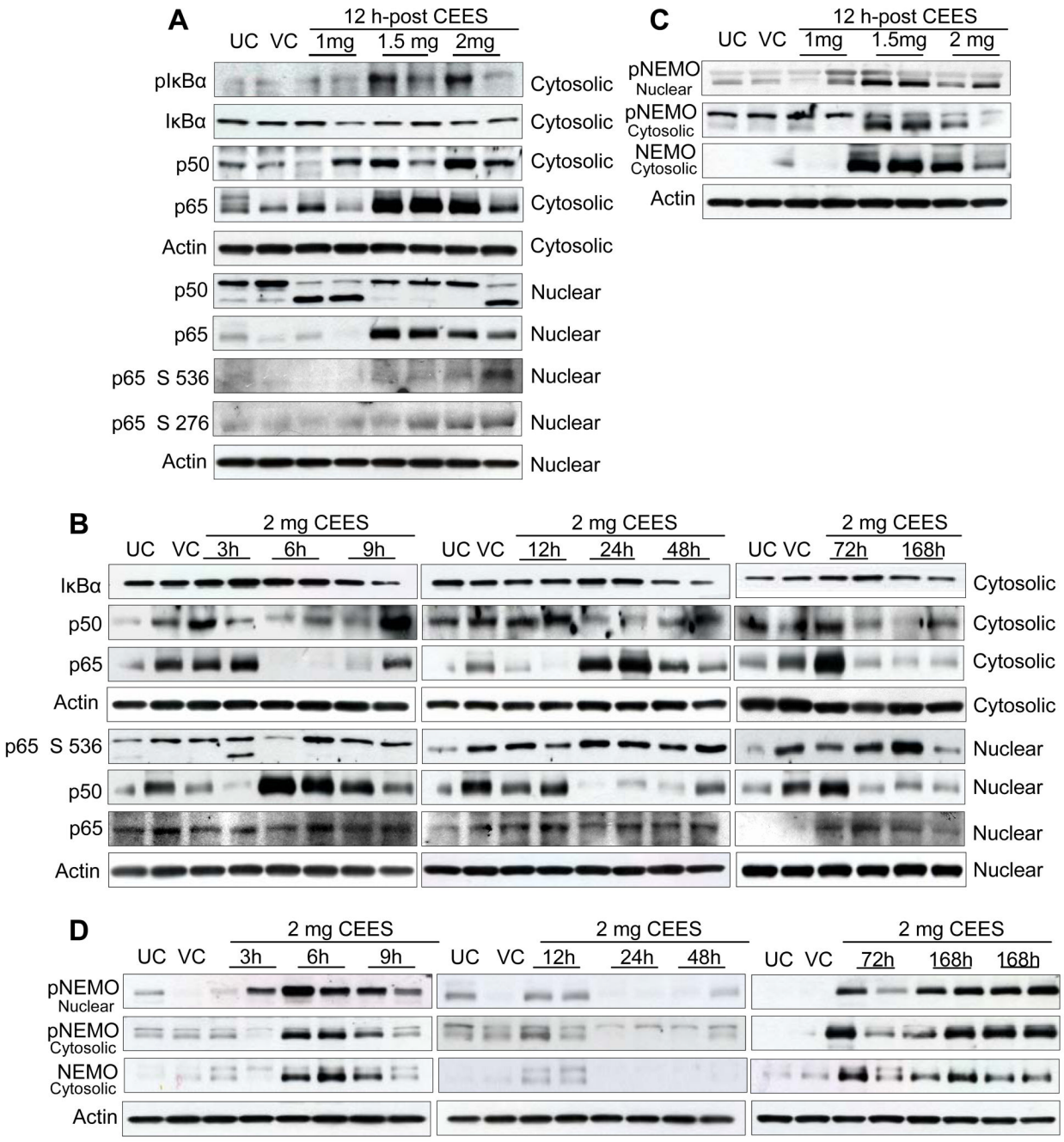

Fig. 9.

Effect of topical CEES exposure on phosphorylation of NEMO and an activation of NF-κB in SKH-1 hairless mouse skin. Mice were treated topically with different doses of CEES or acetone alone, and the dorsal skin was collected at specific time points as detailed under Materials and Methods. Nuclear and cytosolic lysates as required, from mouse skin, were analyzed by western blot for phospho-IκBα, p65 and total IκBα, p65 and p50 (A), phospho-NEMO and total NEMO (C) in dose-response study post 12 h treatment. In time-response study, employing 2 mg CEES, western blot analysis was carried out similarly for phospho-IκBα, p65 and total IκBα, p65 and p50 (B) and phospho-NEMO and total NEMO (D) as described under Materials and Methods. The membranes were stripped and reprobed with β-

actin as a loading control. The results are representative of two animals in each dose- and time-response study. UC, untreated control; VC, vehicle control.

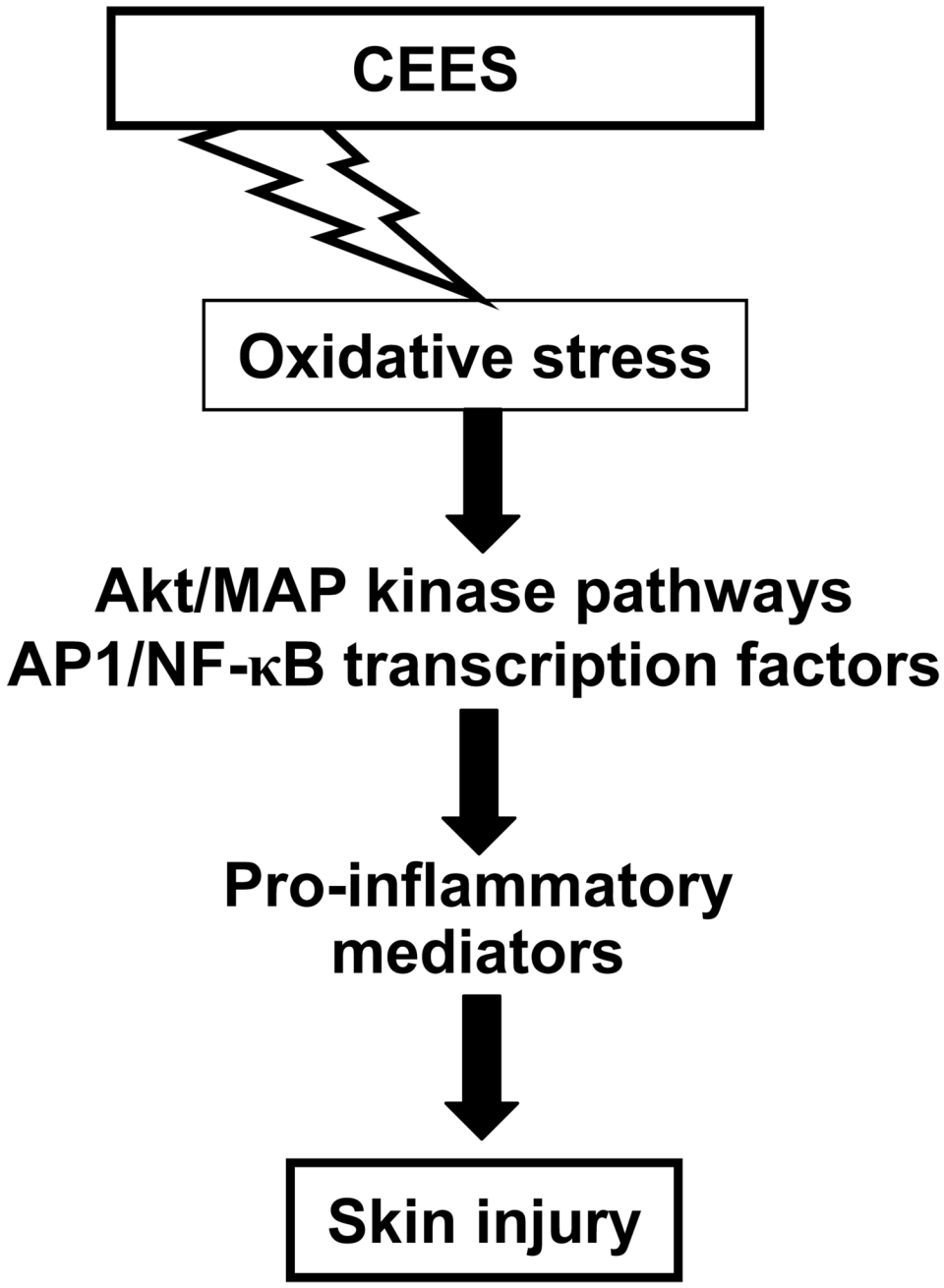

Fig. 10.
Schematic representation of the possible key mechanism of CEES-caused skin injury and inflammation in SKH-1 hairless mouse skin toxicity model.

Table 1

CEES-induced oxidative damage of biological molecules and phosphorylation/activation sequence of key signaling pathways in SKH1 hairless mouse skin[a]

Oxidative stress related damage and signaling pathways	Oxidative damage and activation of signaling molecules following 2 mg CEES exposure of skin compared to controls (time kinetics)							
Oxidative damage and signaling pathways important molecules/proteins)	**3 h**	**6 h**	**9 h**	**12 h**	**24 h**	**48 h**	**72 h**	**168 h**
A. Lipid peroxidation	+	+	+	+	+	+	+	+
B. DMPO nitrone adducts & Protein oxidation	+	+	+	+	+	+	+	+
C. DNA oxidation	−	+	+	+	+	+	+	ND
D. MAPKs								
1. ERK1/2	+	+	+	+	+	+	+	+
2. p38	−	+	+	+	+	+	+	+
3. JNK1/2	−	−	−	+	+	+	+	−
E. PDK1-AKT								
1. PDK1	+	+	+	+	+	+	+	−
2. AKT	−	+	+	+	+	+	+	−
F. AP1 transcription factor								
1. cFos	+	+	+	+	+	+	+	+
2. cJun	+	+	+	+	+	+	+	+
3. ATF-2	+	+	+	+	+	+	+	+
G. NFκB transcription factor	+	+	+	+	+	+	−	−

[a]No visible change (−) or increase (+) in lipid peroxidation, protein and DNA oxidation (A–C), and phosphorylation/activation (D–G) following 2 mg CEES exposure of skin as a function of time (3–168 h) compared to untreated control skin samples. ND, not determined.